

A Review of Physics Models in the LAHETTM Code

R. E. Prael
Los Alamos National Laboratory
Los Alamos, NM, USA

Published in: *Intermediate Energy Nuclear Data: Models and Codes, Proceedings of a Specialists' Meeting*, Issy-les-Moulineaux (France), 30 May-1 June 1994, p. 145, OECD (1994).

Abstract

This paper discusses the various physics options available in LAHET, including the Bertini and ISABEL intranuclear cascade models, the multistage. multi-step preequilibrium exciton model, and the level density parameter options. The interdependence, the interaction with evaporation/fission models, and the sensitivity of results to the choice of options is shown. The particular options used in the code comparison benchmark calculations are compared with the other options possible.

1. Introduction

LAHETTM is a Monte Carlo code for the transport and interaction of nucleons, pions, muons, light ions, and antinucleons in complex geometry¹; it may also be used without particle transport to generate particle production cross sections. It (and all the other variants of HETC) play a significant role in design studies for particle beams with energies in the range of perhaps 150 MeV to a few GeV (and above, with high energy physics augmentation).

This paper discusses the various physics options in LAHET, their interdependence, and the sensitivity of results to the choice of options. The particular options used in the benchmark calculations submitted for comparison² are identified.

The benchmark results originally submitted, and subsequently published², were incorrect; as a result of error, the LAHET results correspond to incident *neutrons* rather than incident protons. A new contribution has been prepared and submitted for these transactions³. A complete tabulation of the proper calculated results is available from the author.

2. Intranuclear Cascade Model Options

The Bertini model⁴ (from HETC) describes the nucleon-nucleus interaction below 3.5 GeV and the pion-nucleon interaction below 2.5 GeV; a scaling law approximation is used to continue the interaction energy to arbitrarily high energies, although a reasonable upper limit is about 10 GeV. The Bertini INC is the default option in LAHET, **and has been used in these code intercomparisons.**

As an alternative to the Bertini intranuclear cascade model, LAHET contains the INC routines from the ISABEL code. The ISABEL INC model is an extension by Yariv and Fraenkel⁵ of the VEGAS code⁶. It has the capability of treating nucleus-nucleus interactions as well as particle-nucleus interactions. It allows for interactions (“CAS-CAS”) between particles both of which are excited above the Fermi sea⁷. The nuclear density is represented by up to 16 density steps, rather than three as in the Bertini INC. It also allows antiproton annihilation⁸, with emission of kaons and pions. As presently implemented in LAHET, only projectiles with $A \leq 4$ are allowed, and antiproton annihilation is not presently allowed in particle transport problems. The upper incident energy limit is 1 GeV per nucleon. Running time is generally 5 - 10 times greater per collision than with the Bertini model.

The ISABEL model contains many optional features; a knowledgeable user

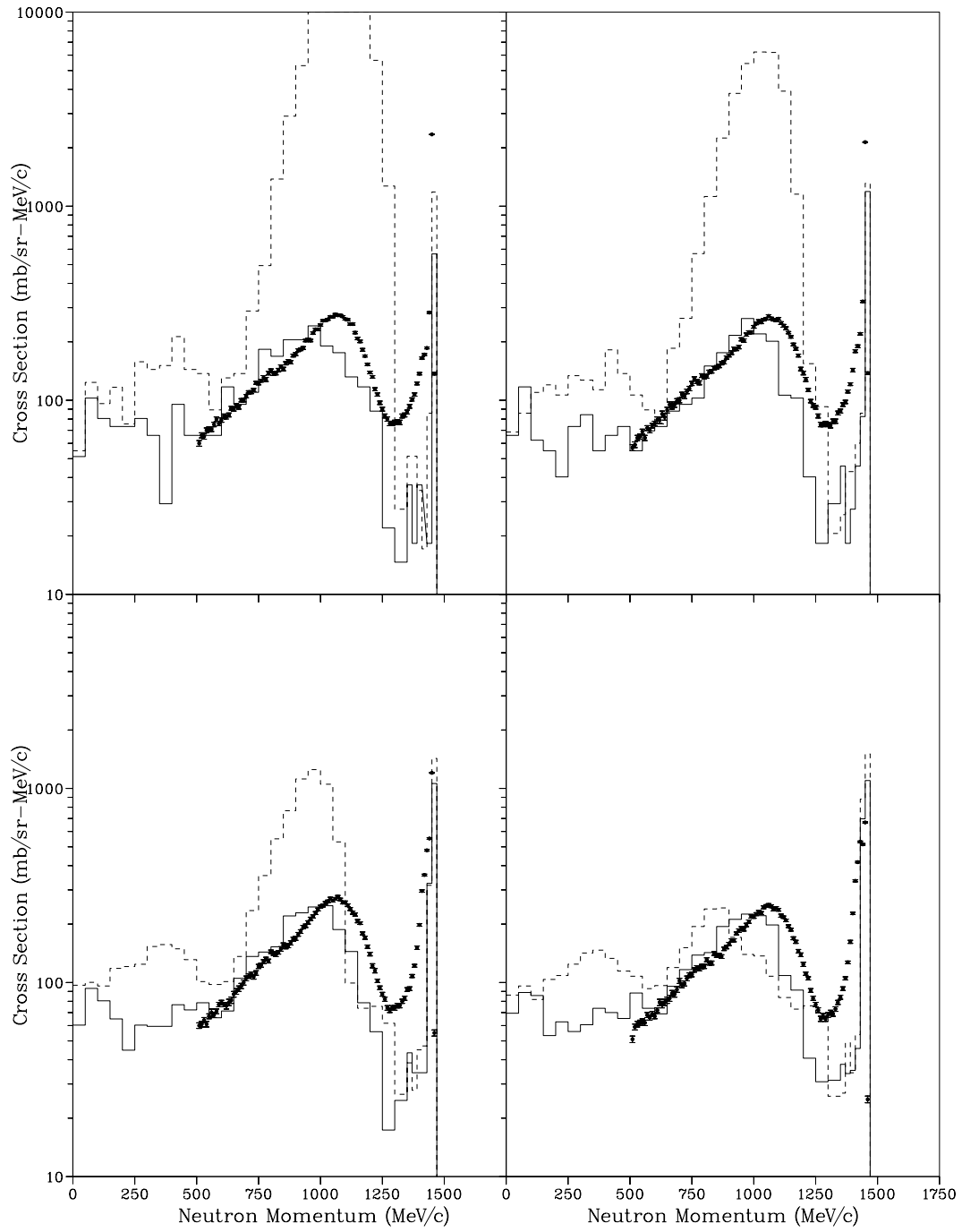


Figure 1: 800 MeV protons on ${}^7\text{Li}$ Calculations with ISABEL INC (solid line) and Bertini INC (dashed line); data from Jeppesen⁹. Upper left: neutron emission spectrum at 0° . Upper right: spectrum at 1° . Lower left: spectrum at 3° . Lower right: spectrum at 4° .

is awaited who would benchmark (and perhaps debug!) many of these features. The option has rarely been used in production calculations, since the Bertini model is considered adequate for most design applications, and advantages of the ISABEL model are frequently too subtle to be considered important in practical problems.

In figure 1, we see a comparison of Bertini and ISABEL results are very small angles, with ${}^7\text{Li}(p, xn)$ data by Jeppesen⁹. The distortion in the Bertini model angular distributions at small angles is well known, but this example displays it very clearly. The ISABEL model performs very well even at the smallest angles, apart from the narrowness of the quasielastic peak. The forward angle distortion for the Bertini model is not normally observed; for these benchmark calculations, the “0° ” calculation is actually an average over the interval 0° to 5.1° , so that the defect is largely unobservable due to the small solid angle at which it appears. **3. Level Density Parameter Options**

The default evaluation of the level density parameter a uses the energy dependent formulation of Ignatyuk¹⁰ as implemented in GNASH¹¹, with the provision that

$$\lim_{E \rightarrow 0} a(E) = a_0$$

where E is the excitation energy and a_0 is Gilbert-Cameron-Cook level density parameter. The low- and high-excitation limits are shown in figure 2. The full energy dependence is used in the preequilibrium model; for the evaporation model, a constant value is taken at an excitation energy near the most likely excitation of the nucleus after the evaporation process. **The default level density model has been used for the intercomparison calculations.**

LAHET includes two other models for the level density parameter. One is the mass dependent model developed for the Jülich version of HETC¹³. As illustrated in figure 2, it closely follows the GCC values for stable nuclei. In LAHET, it is applied as original formulated, independent of energy, but *could* be used as the low-excitation limit in the Ignatyuk model.

The other option is the mass and isospin dependent model originally used in the evaporation model of HETC¹³:

$$a = A(1 + y_0(A - 2Z)^2)/b_0$$

where the default values $b_0 = 8.0$ and $y_0 = 1.5$ may be changed by the user. An example of the HETC level density option is shown in figure 3, along with the Jülich model and guide lines corresponding to $A/8$, $A/10$, and $A/14$.

4. The Preequilibrium Model

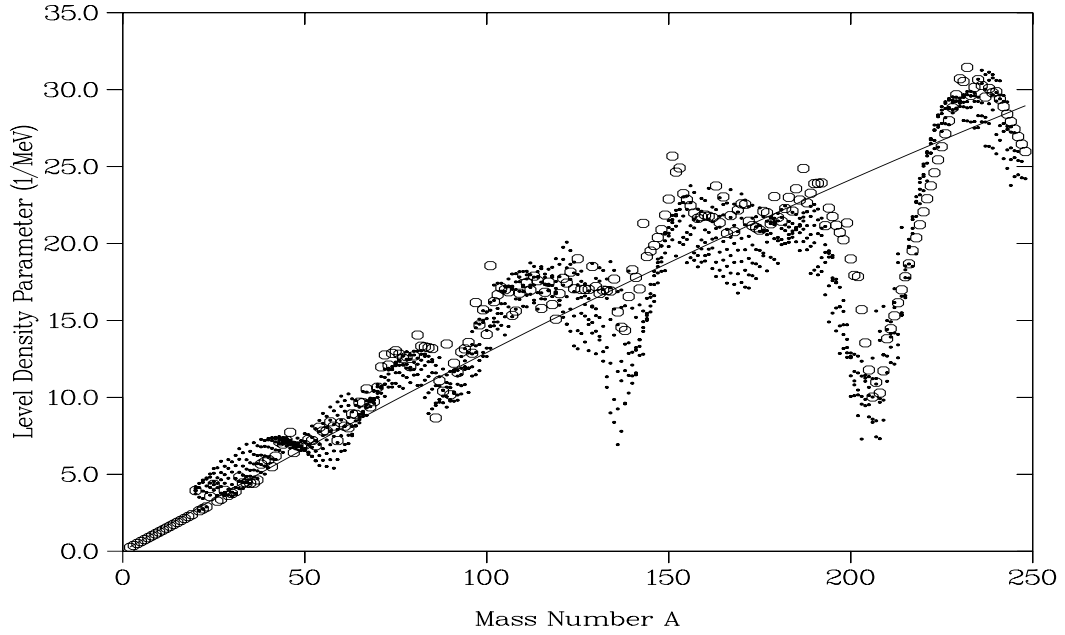


Figure 2: Level density parameters. The points are Gilbert-Cameron-Cook values for masses near the line of stability; the line is the Ignatyuk high excitation limit. The circles are the Jülich mass dependent model.

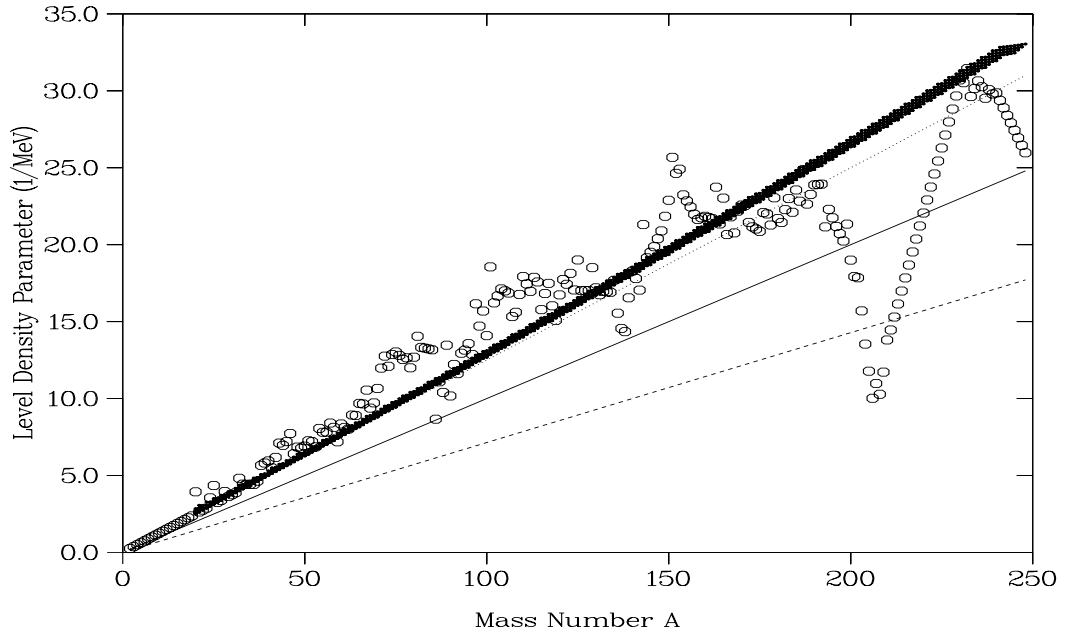


Figure 3: Level density parameters. The points are typical values for the original HETC mass and isospin dependent model for masses near the line of stability. The circles are the Jülich mass dependent model. For comparison, the lines are $A/8$ (dot), $A/10$ (solid), and $A/14$ (dash).

Subsequent deexcitation of the residual nucleus may optionally employ a multistage, multistep preequilibrium exciton model¹⁴ (“MPM”). The MPM is invoked at the completion of the INC, with an initial particle-hole configuration and excitation energy determined by the outcome of the cascade. At each stage in the MPM, the excited nucleus may emit a neutron, proton, deuteron, triton, ^3He , or alpha; alternatively, the nuclear configuration may evolve toward an equilibrium exciton number by increasing the exciton number by one particle-hole pair. The MPM terminates upon reaching the equilibrium exciton number; the evaporation model (or the Fermi breakup model) is then applied to the residual nucleus with the remaining excitation energy.

In the implementation of the MPM, the inverse reaction cross sections are represented by the parameterization of Chatterjee¹⁵. The potentials from which the inverse reaction cross sections are obtained are those selected by Kalbach¹⁶ for the PRECO-D2 code.

When the ISABEL intranuclear cascade model is invoked, it is possible to determine explicitly the particle-hole state of the residual nucleus since a count of the valid excitations from the Fermi sea (and the filling of existing holes) is provided. To define the initial condition for the MPM, the number of particle-hole pairs is reduced by one for each intranuclear collision for which both exiting nucleons are below the top of the nuclear potential well. This method is the only option implemented in LAHET to link the MPM with the ISABEL INC.

In adapting the MPM to the Bertini INC, it has not been possible yet to extract the same detailed information from the intranuclear cascade history. Consequently, the algorithm which defines the interface between the Bertini INC and the MPM is a rather crude approximation, intended to permit initial evaluation of the MPM but open to further improvement. In this case, the initial condition for the MPM is one particle-hole pair beyond the *minimum* particle-hole configuration allowed by the outcome of the intranuclear cascade. As will be seen below, the adaptive algorithm used with the ISABEL INC is quite effective. However, with the initial condition algorithm used with the Bertini INC, the user has a choice of invoking the MPM in one of three optional modes (or not at all):

1. the MPM continues from the final state of the INC with the initial condition defined as above (“normal MPM”);
2. the INC is used only to determine that an interaction has occurred and the MPM proceeds from the compound nucleus formed by the absorption of the incident particle (“pure MPM”);

3. a random selection is made of one of the above modes at each collision with a probability $P = \min[E_1/E_c, 1.0]$ of choosing the “pure MPM” mode, where E_c is the incident energy and $E_1 = 25\text{MeV}$ (“hybrid MPM”).

In the following examples, we will see several cases which show the sensitivity of the subsequent evaporation/fission stage to the choice of the MPM option. **The hybrid MPM option has been used for the intercomparison calculations.**

5. The Fission Models

LAHET includes as user options two models for fission induced by high energy interactions: the ORNL model¹⁷, and the Rutherford Appelton Laboratory (RAL) model by Atchison¹⁸; the fission models are employed with the evaporation model. The RAL model allows fission for $Z \geq 71$, and is the default fission model in LAHET. The RAL model really is two models, for actinide and for subactinide fission.

The data from neutron-induced fission experiments performed at Los Alamos National Laboratory over the energy range 15 MeV to 400 MeV is nearing publication¹⁹. The fission cross section ratio data (relative to ^{235}U) will provide excellent benchmarking opportunities for the fission models used in LAHET and other codes for many actinides.

Figures 4 and 5 compare the Bertini INC/RAL fission and the ISABEL INC/RAL fission models, for various MPM options, with the data¹⁹ for the fission cross section for neutrons on ^{235}U . For the Bertini model cases, the choice of MPM option appears to make no more than a 5% difference. The cases using the ISABEL model are more sensitive to the MPM option at low energies, and less at higher energies. In the region where we expect the most reliable results (above 100 MeV), both MPM options with the ISABEL INC show a better match than the Bertini cases. One must note that the discrepancy at low energy may be largely due to the fact that the reaction (nonelastic) cross section calculated with either INC option does not track the data well; the best test of the fission model would be benchmarking the fission yield (as a fraction of the nonelastic cross section).

Figure 6 illustrate the use of the subactinide fission routines of the RAL model for neutron-induced fission in ^{208}Pb ²⁰. The effect of the MPM is very evident. The calculated cross section is very low even without the preequilibrium model, and the use of the MPM reduces it still further. The is sensitivity to the INC model, even without the use of the MPM. Results using the HETC

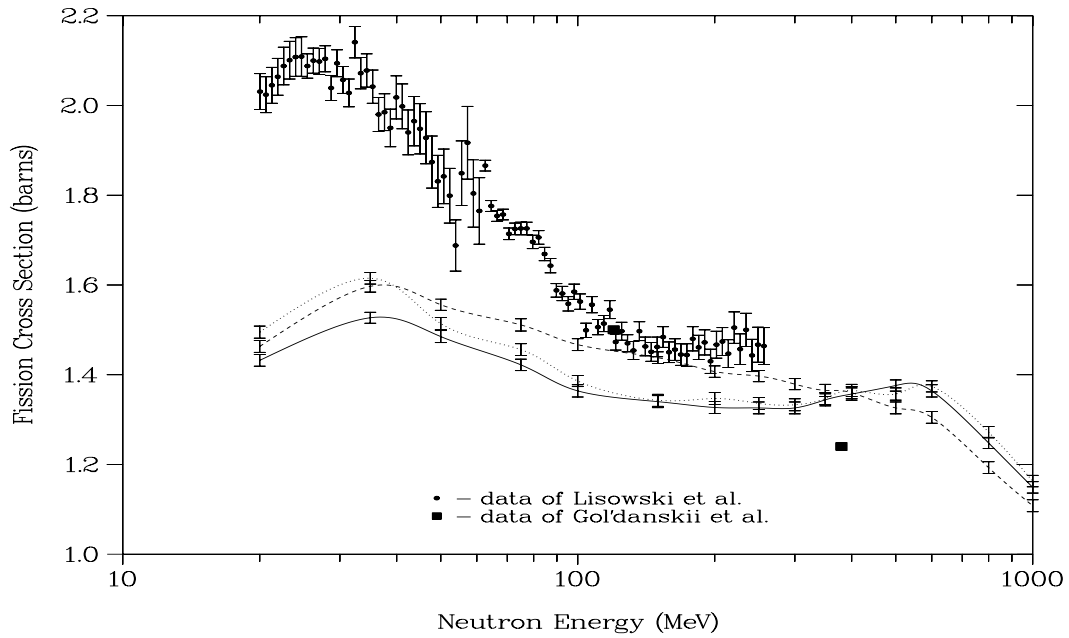


Figure 4: Neutron induced fission cross section for ^{235}U , using the Bertini INC, the RAL fission model, and the default level density model. Solid line: standard MPM. Dashed line: no MPM. Dotted line: hybrid MPM.

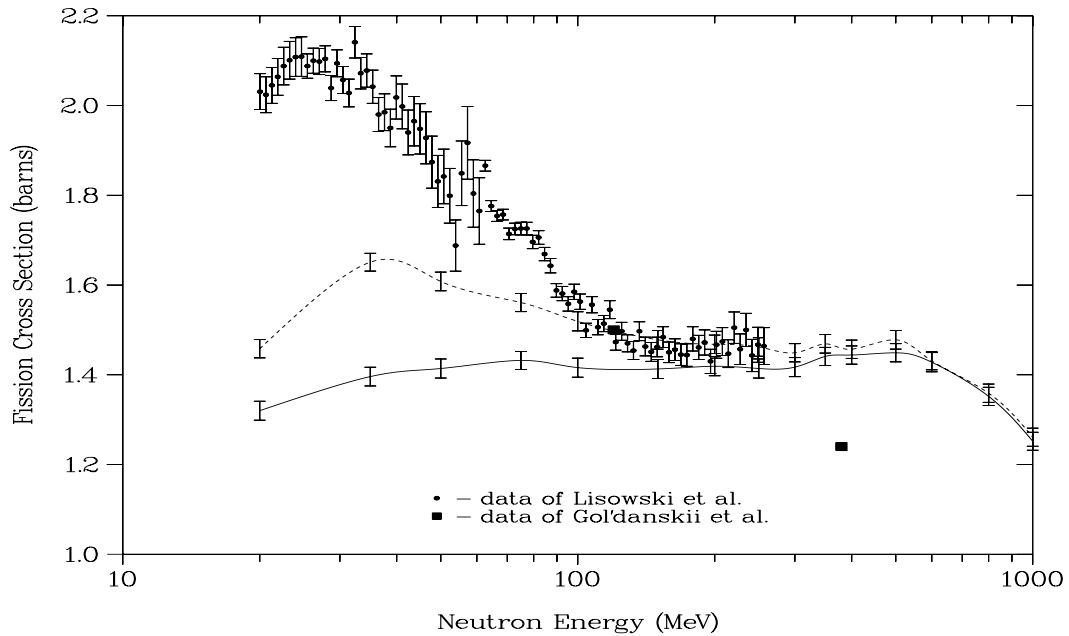


Figure 5: Neutron induced fission cross section for ^{235}U , using the ISABEL INC, the RAL fission model, and the default level density model. Solid line: standard MPM. Dashed line: no MPM.

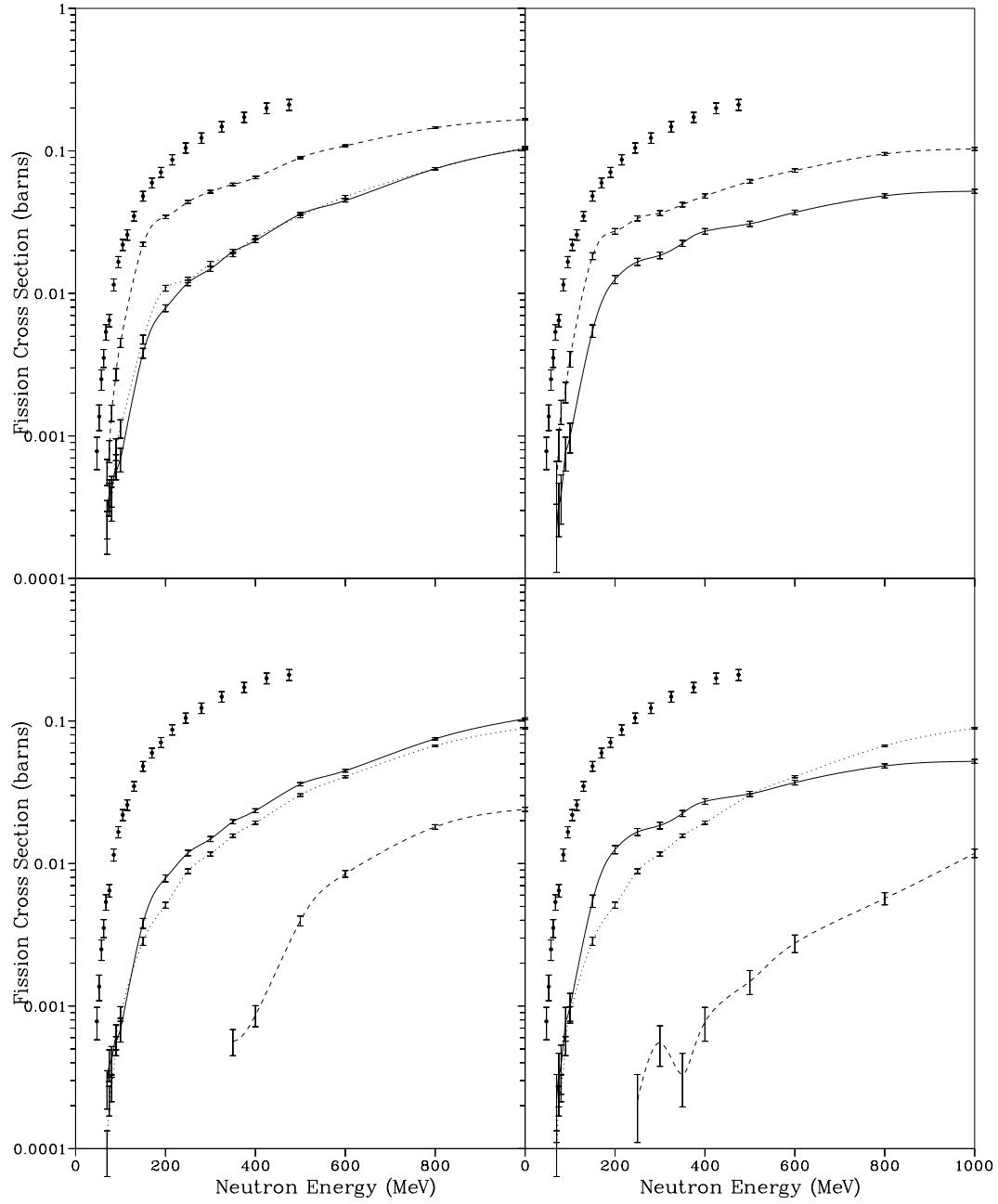


Figure 6: Neutron induced fission cross section for ^{208}Pb , with data of Vonach et al. Upper left: Bertini INC, RAL fission, and default level density; solid - standard MPM, dash - no MPM, dot - hybrid MPM. Upper right: ISABEL INC, RAL fission, and default level density; solid - standard MPM, dash - no MPM. Lower left: Bertini INC, RAL fission, and standard MPM; solid - default level density, dash - Julich level density, dot - HETC level density ($B0 = 10.0$). Lower right: same as lower left, but with ISABEL INC.

level density model with $B_0 = 10.0$ are quite close to those using the default level density model, but using the Jülich level in conjunction with the MPM exaggerates the discrepancy even further. These results strongly indicate that more attention should be devoted to developing a subactinide fission model, consistent with the use of the preequilibrium model, adapting a better treatment from some other code, or attempting to adjust the current model.

6. Additional Features

In LAHET, the Fermi breakup model²¹ has replaced the evaporation model for the disintegration of light nuclei; it treats the deexcitation process as a sequence of simultaneous breakups of the excited nucleus into two or more products, each of which may be a stable or unstable nucleus or a nucleon. Any unstable product nucleus is subject to subsequent breakup. The probability for a given breakup channel is primarily determined from the available phase space, with probabilities for two-body channels modified by Coulomb barrier, angular momentum, and isospin factors. The model is applied only for residual nuclei with $A \leq 17$, replacing the evaporation model for these nuclei. In the LAHET implementation, only two- and three-body breakup channels are considered; it is an abbreviated form of a more extensive implementation of the Fermi breakup model, with up to 7-body simultaneous breakup, used previously for cross section calculations on light nuclei²².

LAHET differs from HETC in the use of cutoff energies for particles escaping from the nucleus during the intranuclear cascade. For either INC model, the neutron cutoff energy is uniformly distributed between zero and *twice* the mean binding energy. The Coulomb barrier is randomly distributed in a form simulating a Coulomb barrier transmission probability; the maximum of the Coulomb barrier and the neutron cutoff is then used as the proton cutoff. The sampling for the cutoff energies is performed once for each projectile-target interaction; the barriers thus defined are then applied to every particle emission in the resulting cascade. This procedure, admittedly artificial, has the effect of preventing a discontinuity in the particle emission spectrum while preserving quite well the mean particle emission rates.

Another small addition to the intranuclear cascade procedure is applied to (p,n) and (n,p) INC reactions only. In this case, the outgoing particle energy is corrected by the binding energy difference in the entrance and exit channels. The modification greatly improves the realism in the high energy emission spectrum and significantly improves the overall energy balance in the INC.

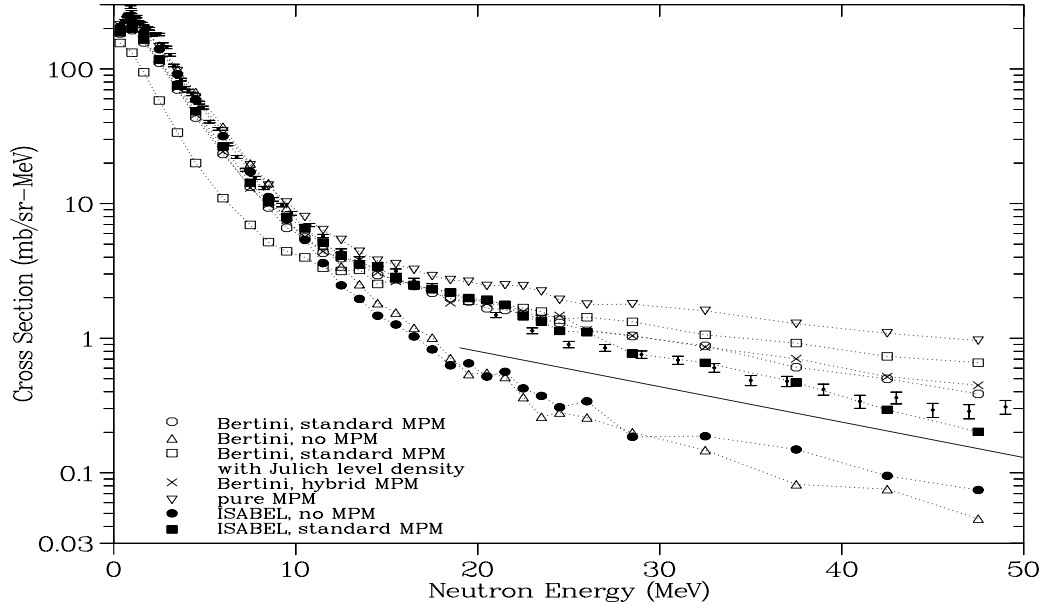


Figure 7: Neutron emission spectrum at 150° for 256 MeV protons on natural Pb. Data points are those of Meier, et. al.²³; solid line is fit to data of Stamer et. al.² The default level density is used, except as noted.

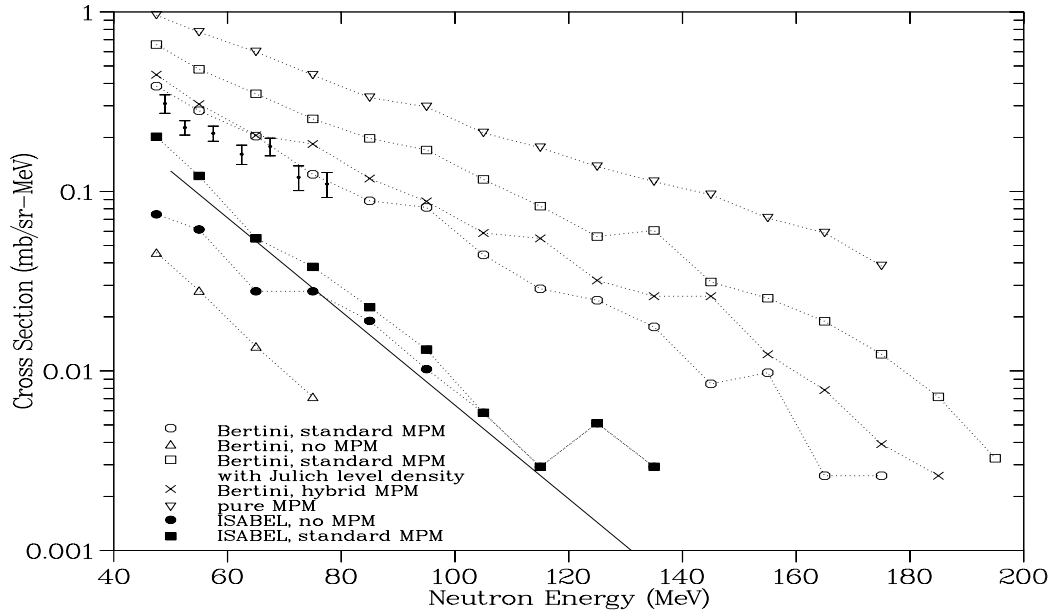


Figure 8: Neutron emission spectrum at 150° for 256 MeV protons on natural Pb. Data points are those of Meier, et. al.²³; solid line is fit to data of Stamer et. al.² The default level density is used, except as noted.

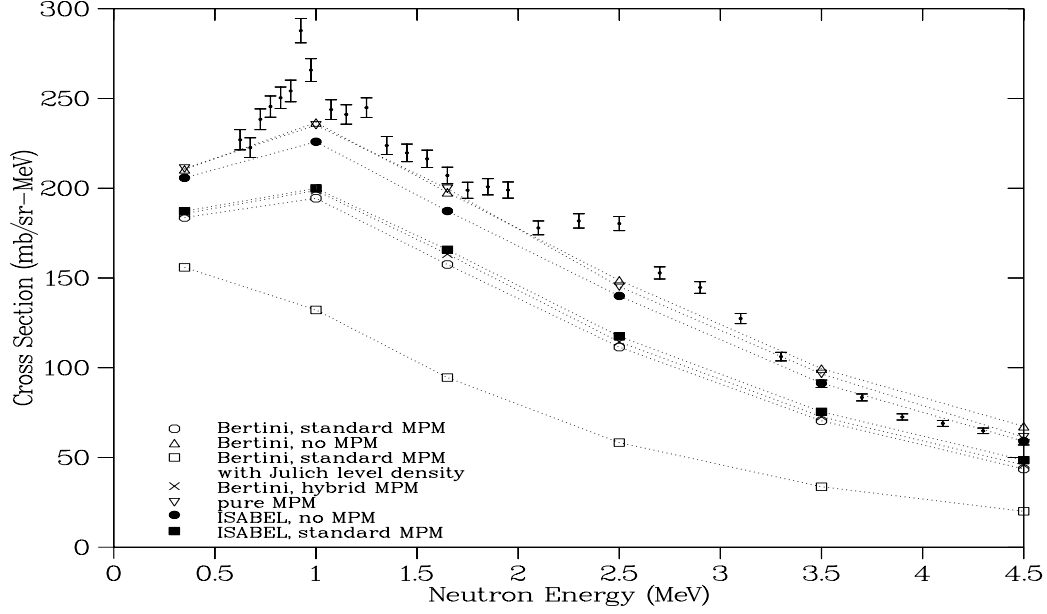


Figure 9: Neutron emission spectrum at 150° for 256 MeV protons on natural Pb. Data points are those of Meier, et. al.²³ The default level density is used, except as noted.

7. A Case Study: Neutron Spectrum at 150° for 256 MeV Protons on Natural Pb.

In figures 7, 8, and 9, the double differential neutron production cross section for 256 MeV protons on natural lead is shown for all the combinations of INC and MPM options (and for one case with the Jülich level density rather than the default). The data points shown are the older data of Meier used in a previous LAHET benchmark report²³. A fitted solid line represents the data of Stamer included in the report² on the comparison calculations. Calculated points using the models chosen for the comparison are marked by “X”.

In figure 7, we see that all the Bertini model calculations with MPM lie above the ISABEL MPM results, and above all the data. In this energy range, below 50 MeV emission energy, the ISABEL MPM agrees well with the older data but is approaching the newer. Both cases without the MPM are well below the data. The use of the Jülich level density exaggerates emission from the MPM and consequently depletes emission from the evaporation phase.

In figure 8, above 50 MeV, the ISABEL results approach the newer data,

while the Bertini results with MPM are high. In this context, the new data would indicate that the ISABEL model to be superior (as one would expect). The fact that the ISABEL results appear to converge seems to indicate that the back angle emission at higher energies comes from the INC model, not the MPM phase.

In figure 9, we see the detail around the evaporation peak. Note that the pure MPM case and the no MPM cases give almost the same contribution in the energy range. The two INC models with the standard or hybrid INC give essentially the same low energy spectrum. The effect of the Jülich level density is as noted with respect to figure 7 and parallels the effect on the calculated neutron induced fission cross section discussed in section 5.

8. Conclusions

From an examination of the new calculations submitted for the code comparison, using the Bertini INC, the hybrid MPM, and the default level density model, some conclusions may be drawn as stated in the calculational summary³.

Since LAHET conserves energy with respect to real target masses for quasielastic events, the high energy edge of the (p,xn) cross sections vanishes at the proper energy. The use of the hybrid MPM option eliminates the INC quasielastic peak at low energies, which is desirable, but it appears in its typical over-narrow form as the incident energy increases.

However, the coupling of the MPM with the Bertini model in general leads to too much preequilibrium emission, observed at the back angles (see figure 8). This effect results from using a minimally low exciton state as the initial condition for the MPM following the cascade phase, and could be improved with a more sophisticated algorithm.

Another defect may be noted, in that back angle emission from the MPM is nearly uniform at angles from 120° to 180° . As presently coded, the Kalbach systematics are applied to the angular distribution of the emitted particle only for first stage emission; isotropic (C of M) emission is used otherwise. Thus, the anisotropic distribution is employed only when *no* particle is emitted in the cascade phase.

In addition, it is apparent that the subactinide fission model currently used in LAHET is inconsistent with the use of the MPM as currently implemented. The Jülich level density model would probably give comparable results were it used as the low excitation limit of the Ignatyuk formulation; further bench-

marking should be able to show whether that is worthwhile modification.

It would be most desirable to issue a benchmark report using the same data as in the comparison², but displaying the various LAHET options as in figures 7, 8, and 9. Such an effort could be used as a guide for further development, as well as a guide for the user.

9. References

1. Richard E. Prael and Henry Lichtenstein, "User Guide to LCS: The LAHET Code System", LA-UR-89-3014, Los Alamos National Laboratory (September 1989).
2. M. Blann et. al., *International Code Comparison for Intermediate Energy Nuclear Data*, Nuclear Energy Agency, OECD, Paris (1994).
3. R. E. Prael, "LAHETTM Benchmark Calculations for Protons Incident on ⁹⁰Zr and ²⁰⁸Pb", submitted for *Specialists' Meeting on Intermediate Energy Nuclear Data*, Nuclear Energy Agency, OECD, Paris, May 30 - June 1, 1994, LA-UR-94-1796, Los Alamos National Laboratory (May 1994).
4. H. W. Bertini, *Phys. Rev.* **188** (1969), p. 1711.
5. Y. Yariv and Z. Fraenkel, *Phys. Rev. C*, **20** (1979), p. 2227.
6. K. Chen et al., *Phys. Rev.*, **166** (1968), p. 949.
7. Y. Yariv and Z. Fraenkel, *Phys. Rev. C*, **24** (1981), p. 488.
8. M. R. Clover, R. M. DeVries, N. J. DiGiacomo, and Y. Yariv, *Phys. Rev. C*, **26** (1982), p. 2138.
9. R. G. Jeppesen, PhD thesis, U. of Colorado (1986).
10. A. V. Ignatyuk, G. N. Smirenkin, and A. S. Tishin, *Sov. J. Nucl. Phys.* **21** (1975), p. 256.
11. E. D. Arthur, "The GNASH Preequilibrium-Statistical Model Code", LA-UR-88-382, Los Alamos National Laboratory (February 1988).
12. P. Cloth et al., "The KFA-Version of the High-Energy Transport Code HETC and the Generalized Evaluation Code SIMPEL", Jül-Spez-196, Kernforschungsanlage Jülich GmbH (March 1983).
13. L. Dresner, "EVAP - A Fortran Program for Calculating the Evaporation of Various Particles from Excited Compound Nuclei", ORNL-TM-196, Oak Ridge National Laboratory (April 1962).

14. R. E. Prael and Michael Bozoian, "Adaptation of the Multistage Preequilibrium Model for the Monte Carlo Method", LA-UR-88-3238, Los Alamos National Laboratory (September 1988).
15. A. Chatterjee, K. H. N. Murthy, and S. K. Gupta, *Pramāna* 16 (1981), p. 391.
16. C. Kalbach, "PRECO-D2: Program for Calculating Preequilibrium and Direct Reaction Double Differential Cross Sections", LA-10248-MS, Los Alamos National Laboratory (1985).
17. J. Barish et al., "HETFIS High-Energy Nucleon-Meson Transport Code with Fission", ORNL/TM-7882, Oak Ridge National Laboratory (1981).
18. F. Atchison, "Spallation and Fission in Heavy Metal Nuclei under Medium Energy Proton Bombardment", in *Targets for Neutron Beam Spallation Sources*, Jül-Conf-34, Kernforschungsanlage Jülich GmbH (January 1980).
19. P. W. Lisowski, Los Alamos National Laboratory (unpublished).
20. H. Vonach et al., (unpublished).
21. D. J. Brenner, R. E. Prael, J. F. Dicello, and M. Zaider, "Improved Calculations of Energy Deposition from Fast Neutrons", in *Proceedings Fourth Symposium on Neutron Dosimetry*, EUR-7448, Munich-Neuherberg (1981).
22. D. J. Brenner and R. E. Prael, "Calculated Differential Secondary-particle Production Cross Sections after Nonelastic Neutron Interactions with Carbon and Oxygen between 10 and 60 MeV", *Atomic and Nuclear Data Tables* 41,71-130 (1989).
23. R. E. Prael, "LAHET Benchmark Calculations of Differential Neutron Production Cross Sections for 113 MeV and 256 MeV Protons", LA-UR-89-3347, Los Alamos National Laboratory (September 1989).

LAHETTM is a trademark of the Regents of the University of California and the Los Alamos National Laboratory.